Nuclear Engineering and Technology xxx (2018) 1–7

Contents lists available at ScienceDirect

Nuclear Engineering and Technology

journal homepage: www.elsevier.com/locate/net

Original Article

Thermal transport in thorium dioxide

Jungkyu Park*, Eduardo B. Farfán, Christian Enriquez

Kennesaw State University, Department of Mechanical Engineering, Kennesaw, GA 30144, USA

ARTICLE INFO

Article history:
Received 28 September 2017
Received in revised form
20 December 2017
Accepted 12 February 2018
Available online xxx

Keywords:
Molecular Dynamics Simulation
Nuclear Fuel
Thermal Transport
Thorium Dioxide

ABSTRACT

In this research paper, the thermal transport in thorium dioxide is investigated by using nonequilibrium molecular dynamics. The thermal conductivity of bulk thorium dioxide was measured to be 20.8 W/m-K, confirming reported values, and the phonon mean free path was estimated to be between 7 and 8.5 nm at 300 K. It was observed that the thermal conductivity of thorium dioxide shows a strong dependency on temperature; the highest thermal conductivity was estimated to be 77.3 W/m-K at 100 K, and the lowest thermal conductivity was estimated to be 4.3 W/m-K at 1200 K. In addition, by simulating thorium dioxide structures with different lengths at different temperatures, it was identified that short wavelength phonons dominate thermal transport in thorium dioxide at high temperatures, resulting in decreased intrinsic phonon mean free paths and minimal effect of boundary scattering while long wavelength phonons dominate the thermal transport in thorium dioxide at low temperatures.

1. Introduction

The utilization of thorium as a new energy source has been of interest to researchers for several years [1]. Thorium exists in nature as Th-232 and is more abundant than uranium, which has been the typical nuclear fuel. Thorium is fertile and must be converted into fissile material (nuclear fuel) via a breeding process accomplished by neutron absorption in a nuclear reactor and subsequent nuclei conversions [1,2]. The resulting fissile U-233 can be used in any of several kinds of national or international nuclear reactors [1,3,4].

Thorium oxide (ThO_2), also known as thoria, has one of the highest melting points among all oxides (3573.15 K) [5]. Consequently, ThO_2 is used in light bulbs, arc-light lamps, welding electrodes, and heat-resistant materials [6–8]. As a nuclear fuel, ThO_2 has several advantages when compared to conventional uranium-based fuels. ThO_2 is relatively inert and has lower thermal expansion than UO_2. Fission gas release from ThO_2 nuclear fuel pellets is much lower than that from UO_2. In particular, its high thermal conductivity makes ThO_2 a better fuel for nuclear reactors since thermal transport is a critical issue that is directly related to the lifetime of nuclear fuels. There are several types of reactors where ThO_2 can be used as nuclear fuel: heavy water reactors, high-temperature gas-cooled reactors, boiling water reactors, pressurized water reactors, fast neutron reactors, and molten salt reactors.

The efficient thermal transport property of ThO_2 has been a subject of research for many years. In 1954, Kingery et al. [9] reported the thermal conductivity of several oxide materials including ThO_2. In 1969, Murabayashi et al. [10] reported the thermophysical properties of ThO_2 such as thermal diffusivity and thermal conductivity. More recently, Pillai and Raj [11] reported the thermal conductivity of ThO_2 using a steady-state axial heat flow comparative apparatus. There are only a few theoretical calculations for the thermal transport property of ThO_2. Ma et al. [12] reported the specific heat and thermal conductivity of ThO_2 using equilibrium molecular dynamics (MD) simulations, but the sample length is limited to 6 unit cells only.

The present study provides a meaningful addition to current literature as it presents microscopic understanding on thermal transport in ThO_2. Using classical MD along with the potential field for actinide oxides developed by Cooper et al [13–15], the thermal conductivity and the phonon mean free path of ThO_2 were obtained in this study. By progressively increasing the sample length up to 200 unit cells, the thermal conductivity of the bulk ThO_2 is estimated. Additionally, to better understand the temperature effect on thermal transport in ThO_2, thermal conductivities are estimated for ThO_2 structures at various temperatures, ranging from 100 K to 1200 K.

2. Simulation method

In this work, reverse nonequilibrium molecular dynamics (RNEMD) is employed to obtain thermal conductivity of ThO_2. The

* *Corresponding author.*
E-mail address: jpark186@kennesaw.edu (J. Park).

https://doi.org/10.1016/j.net.2018.02.002

schematic of the RNEMD simulation is shown in Fig. 1. RNEMD is a MD method for measuring transport property using cause and effect reversed algorithm first introduced by Müller-Plathe [16] and has been constantly used to estimate thermal properties of materials [17–20]. In this study, the RNEMD algorithm implemented in large-scale atomic/molecular massively parallel simulator (LAMMPS) [21] is used to create a heat flux by swapping energy between a hot bath and a cold bath in a simulation box. By the help of the periodic boundary condition, two cold baths are generated at the ends of the simulation box.

To perform RNEMD, the simulation system needs to be well-equilibrated to forget its initial thermodynamic state. Once the simulation structure is properly equilibrated, the simulation box is divided into many imaginary bins along the direction in which the thermal conductivity is to be calculated using the simulation algorithm. During the simulation, energy is swapped at each specified time step by exchanging velocity vectors of the coldest atoms in the hot region and the hottest atoms in the cold region to create a temperature gradient in the simulation structure. Energy exchange between the cold bath and hot bath occurs until the heat flow reaches a steady state. Once the heat flow in the structure reaches a steady state, the thermal conductivity, k, is calculated using the Fourier's heat conduction law with averaged heat flux and temperature gradient dT/dx as the following.

$$k = -\frac{\langle q \rangle}{\langle dT/dx \rangle}, \tag{1}$$

where $\langle q \rangle$ is the heat flux and $\langle dT/dx \rangle$ is the temperature gradient in the sample averaged over time and space. The brackets < >, indicate the average of the quantities over time as well as over the particles in the simulation cell.

The simulation structures (Fig. 1) and LAMMPS input data are constructed by using custom MATLAB programs. It must be noted that thermal transport in these structures is size dependent since phonons with wavelengths longer than the computational unit cells cannot be excited, thus limiting the overall thermal conductivity. However, the effect of simulation box boundary on thermal transport is expected to be diminished continuously as the simulation structure size increases progressively in the direction of thermal conductivity estimation (x direction in the present study) until the size of the simulation structure becomes larger than its intrinsic phonon mean free path.

In all structures simulated, the two side lengths, i.e. L_y and L_z, are constructed to be the same. In the case of ThO_2, three different side lengths ($L_y = L_z$ = 1.12 nm, 3.36 nm, and 5.6 nm) are chosen to investigate the thermal conductivity in x direction; 1.12 nm, 3.36 nm, and 5.6 nm correspond to 2, 6, and 10 unit cells, respectively. The other control parameter, i.e. the sample length, L_x, is defined as the half length of the x-direction length of the simulation structure since the characteristic length for thermal conductivity estimation in RNEMD is the distance between the hot bath located in the middle of the simulation structure and the cold bath located in the ends of the simulation structure; two identical temperature profiles are induced symmetrically after exchanging energy between the hot bath and two cold baths. Eight different sample lengths (L_x = 2.8 nm, 5.6 nm, 11.2 nm, 16.8 nm, 22.4 nm, 28 nm, 42 nm, and 56 nm) are selected for the present study; these eight different lengths are equivalent to 5, 10, 20, 30, 40, 50, 75, and 100 unit cells, respectively.

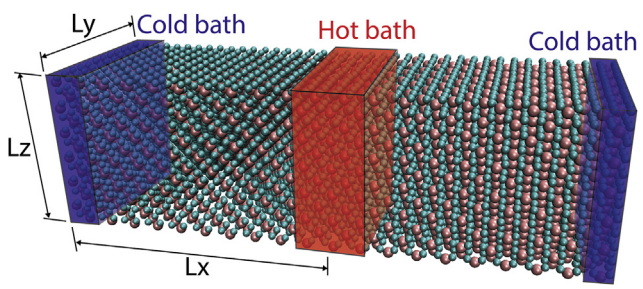

Fig. 1. Schematic of sample preparation for RNEMD.
RNEMD, reverse nonequilibrium molecular dynamics.

UO_2 structures are also constructed for comparison. For the case of thermal conductivity estimation for UO_2, the side length is fixed to be $L_y = L_z$ = 3.28 nm (6 unit cells). The sample lengths, L_x, selected for the thermal conductivity estimation of UO_2 are 5.47 nm, 10.9 nm, 16.4 nm, 21.8 nm, 27.3 nm, 41.0 nm, and 54.7 nm that are equivalent to 10, 20, 30, 40, 50, 75, and 100 unit cells, respectively.

All simulations are performed using the LAMMPS [21] code with the potential model for actinide oxides developed by Cooper and Rushton [13–15], which takes into account many body effects to improve the description of thermophysical properties of actinide oxides. The potential model uses the embedded atom method to allow the inclusion of many body interaction during MD simulations, and its functional consists of pairwise and many body components as follows.

$$E_i = \frac{1}{2}\sum_j \phi_{\alpha\beta}(r_{ij}) - G_\alpha \sqrt{\sum_j \sigma_\beta(r_{ij})}, \tag{2}$$

where E_i is the energy of ith atom with respect to all other atoms, r_{ij} is the distance between ith atom and jth atom, and α and β denote the species of ith atom and jth atom, respectively. The first term in the Eq. (2) represents pairwise interaction between ith atom and jth atom, separated by r_{ij} and it includes long range electrostatic contributions and short range contributions. The short range contributions to the potential energy are based on the potential model developed by Morse [22] and Buckingham [23]. The second term in the Eq. (2) introduces many body perturbation to the pairwise interaction by summing a set of pairwise functions, $\sigma_\beta(r_{ij})$, between ith atom and its surrounding atoms. As can be seen in the Eq. (2), many body perturbation is proportional to the square root of the summation of pairwise functions, where G_σ is the proportionality constant. The detailed information for the functional can be found in Cooper et al. [13]. This potential model has successfully predicted thermophysical properties of actinide solids such as thermal expansion and specific heat capacity [13]. More recently, it has been employed to calculate the diffusion properties of CeO_2, ThO_2, and UO_2 [14,24] as well as the thermal conductivity of UO_2 [25].

The simulation structure is energy-minimized first by iteratively adjusting atomic coordinates to get a near 0 K structure. Once energy-minimization is finished, the temperature is elevated to 500 K using isenthalpic (NPH) ensemble with Langevin thermostat for faster equilibration. Then, the system is cooled down to room temperature with isothermal–isobaric (NPT) ensemble and equilibrated. RNEMD is carried out on the equilibrated structures for 2 ns with micro-canonical (NVE) ensemble with a time-step of 1 fs.

3. Results and discussion

The temperature profile obtained after imposing a heat flux for 2 ns is shown in Fig. 2. The temperature slips at the boundaries result from the unphysical manner by which heat is added/removed at the hot and cold baths [20,26–28]—the continuous discharge of low/high temperature atoms in the hot/cold bath is not compensated timely by the diffusion of low/high temperature atoms from

Please cite this article in press as: J. Park, et al., Thermal transport in thorium dioxide, Nuclear Engineering and Technology (2018), https://doi.org/10.1016/j.net.2018.02.002